

## Reactivity Measurements and Neutron Spectroscopy in the MUSE-4 Experiment

A.Billebaud<sup>\*1</sup>, J.Vollaire<sup>1</sup>, R.Brissot<sup>1</sup>, D.Heuer<sup>1</sup>, C.Le Brun<sup>1</sup>, E.Liatard<sup>1</sup>, J.-M.Loiseaux<sup>1</sup>,  
O.Méplan<sup>1</sup>, E.Merle-Lucotte<sup>1</sup>, A.Nuttin<sup>1</sup>, F.Perdu<sup>1</sup>, C.Destouches<sup>2</sup>, P.Chaussonnet<sup>2</sup>,  
J.-M.Laurens<sup>2</sup>, and Y.Rugama<sup>2</sup>

<sup>1</sup>Laboratoire de Physique Subatomique et de Cosmologie CNRS-IN2P3/UJF,  
53 av. des Martyrs, F-38026 Grenoble, France

<sup>2</sup>CEA Cadarache, DEN/DER/SPEX/LPE, F-13108 Saint-Paul-lez-Durance, France

Reactivity measurement gives access to an important parameter in reactor physics, which can be achieved by many experimental techniques. This paper describes our current efforts to develop and test a method which makes use of the Pulsed Neutron Source technique. To do so, the MASURCA fast neutron reactor was coupled to the pulsed neutron generator GENEPI. For various subcritical configurations, the decay of the neutron population which follows a neutron burst was recorded using in-core fission chambers. The analysis relies on the distribution of time intervals between fission events belonging to the same fission chain. An excellent agreement is found between the measured reactivities and the expected ones, from a near criticality configuration down to very deep subcritical levels. The second part of the paper is devoted to the measurement of the neutron energy distribution. A proportional counter was used to measure the energy deposition of the neutrons in the <sup>3</sup>He active gas. A calibration of the counter response allows us to reconstruct the neutron flux at the detector location. A reasonable agreement is found with a Monte Carlo prediction. This gives us a direct test of the stochastic approach to the neutron transport.

**KEYWORDS:** ADS, subcritical reactor, reactivity monitoring, neutron spectroscopy, <sup>3</sup>He proportional counter

### 1. Introduction

In order to investigate the physical characteristics of a source driven subcritical multiplying medium, a series of experimental investigations has been performed at the CEA Cadarache facility MASURCA, in the frame of the MUSE-4 (MULTiplication of an External Source) program. Among the main objectives of this program are:

- The necessity to improve our knowledge of neutron behavior in a sub-critical medium, by experimentally characterizing the neutron distribution in space, time and energy.
- The definition of experimental methods giving access to the subcriticality level of the assembly without needing to achieve criticality.

The main object of this paper is to present some of the results we obtained as regards the prompt multiplication coefficient measurement and the in core neutron spectroscopy.

### 2. Experimental Setup

During the past 2 years the MASURCA facility has been set-up to perform the MUSE-4

---

\* Corresponding author, Tel. +33 476 28 40 57, FAX +33 476 28 40 04, E-mail: billebaud@lpsc.in2p3.fr

experimental program, including the installation of the pulsed neutron generator GENEPI and its coupling to the reactor assembly. The description of these two facilities can be found elsewhere [1]. We will only review their main characteristics and describe the core configurations we have used.

## 2.1 The MASURCA facility

The MASURCA facility is dedicated to neutronic studies of fast reactor lattices. All the MUSE-4 configurations are based on fuel cell assemblies representative of a fast sodium cooled plutonium core. The core reflector is a stainless steel/sodium blanket. The GENEPI ion guide is located at the core median plane, the tritium target being at the core centre. Three successive subcritical configurations, named SC0, SC2, SC3, were set up by replacing some peripheral fuel cells by stainless steel/sodium cells (see Figure 1). Several complementary configurations were obtained from the previous ones by inserting the pilot rod (“PR down”) which corresponds to a reactivity decrease of roughly 160 pcm<sup>†</sup> as compared to the “PR up” situation.

Reaction rates were measured using <sup>235</sup>U loaded fission chambers, neutron spectroscopy was achieved using <sup>3</sup>He proportional counters. These two types of detectors were inserted vertically in the median plane of the reactor core.

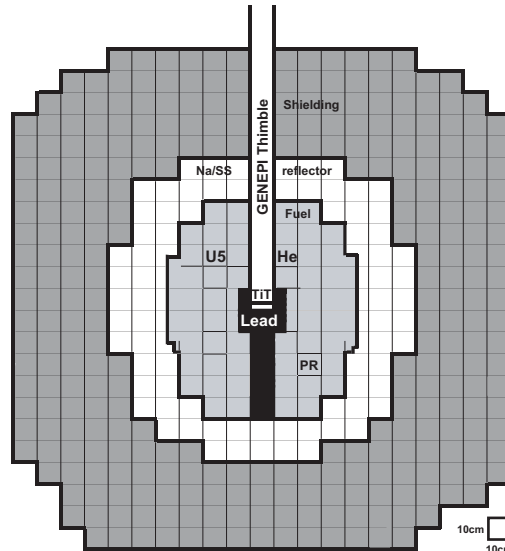


**Fig.1** XY cut of the SC0 subcritical configuration of MASURCA at the median plane, with the detector locations (<sup>235</sup>U and <sup>3</sup>He).

## 2.2 The GENEPI Generator

The external neutron source was provided by a pulsed deuteron accelerator designed for the MUSE-4 experimental program: the GENEPI accelerator. Deuterons are produced by a pulsed duoplasmatron source and accelerated to 220 kV, bent in a magnetic field and then guided onto a tritium target through a glove finger inserted into the reactor core. The width of the deuteron pulse is less than 1 μs and its repetition rate can be adjusted from a few Hertz up to 5 kHz. It provides about  $3 \times 10^6$  neutrons per pulse by T(d,n) reactions.

<sup>†</sup> One pcm unit corresponds to a reactivity of  $10^{-5}$ .

### 3. Prompt Kinetics Measurements

To extract the prompt kinetics parameters we propose a new method based on the analysis of measurements obtained with the Pulsed Neutron Source technique (PNS).

#### 3.1 PNS Raw Data

The method we have selected to characterize the prompt multiplication properties of the sub-critical assembly is based on the measurement of the decay of the neutron population with time, immediately after a neutron pulse produced by the GENEPI generator.

Figure 2 shows the time dependence of the counting rate measured for the three core configurations SC0, SC2, SC3 with the pilot rod inserted into or removed from the core, giving access to six different levels of reactivity. We can see on Figure 2 that the decrease of the counting rate depends strongly on the reactivity level, as expected, and exhibits a sensitivity to reactivity changes as low as 100 pcm.

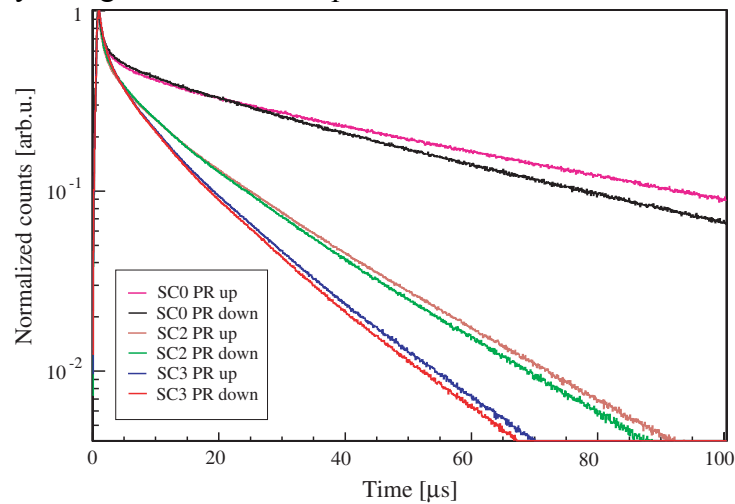


**Fig.2** Neutron population decays for 3 subcritical configurations, with and without the pilot rod insertion.

#### 3.1 Determination of the Prompt Multiplication Coefficient

In an accurate reactor kinetics calculation, it is necessary to consider in detail the space and time dependence of the various cross-sections. The resulting mathematical analysis is necessarily rather complicated. To simplify the calculations, it is generally assumed that the spatial and spectral neutron distributions are constant in time, which implies that all the cross sections entering the analysis are averaged over the flux. This use of average values constitutes the so-called point kinetics (PK) approximation. In the case of a sub-critical medium fed with an external source of neutrons, it leads to an exponential power decrease when the source is switched off. Under this assumption, the decrease rate  $\alpha$ , defined as the logarithmic time derivative of the counting rate, is constant and equal to:

$$\alpha = -\frac{1}{N} \frac{dN}{dt} = \frac{1 - k_p}{l} \quad (1)$$

In this equation  $l$  is the lifetime of the neutron. Thus, if we determine its value by simulation, the multiplication coefficient  $k_p$  can be deduced from an analysis of the counting rate. This approximation is widely used to provide a first estimate of reactor kinetics parameters. However, the real decrease of the neutron population is much more complex: Figure 3 shows

a Monte Carlo simulated distribution  $P(\tau)$  of the time intervals  $\tau$  between neutrons belonging to the same fission chain. We clearly observe a strong departure of the realistic distribution from the PK prediction as early as 15  $\mu\text{s}$  after the birth of the chain triggering neutron. In other words, the logarithmic time derivative of the neutron population,  $\alpha$ , is function of the time elapsed since the feeding of the sub-critical assembly by the neutron pulse. A tracking of the neutrons throughout the whole reactor core highlights the role of the reflector for the presence of numerous fission events some tens of microseconds after the neutron birth: due to the rather low capture cross sections of the reflector materials, neutrons escaping the fuel zone may spend a lot of time in the reflector before coming back into the fuel, thus explaining the slow decrease of the time interval distribution. In order to take into account the full complexity of the multiplication process, we have developed [2] a method based on the use of the intergeneration time distribution  $P(\tau)$ . The first step is to normalize the distribution by computing:

$$P'(\tau) = \frac{P(\tau)}{\int_0^{\infty} P(u) du} \quad (2)$$

In a second step the contribution of each generation is calculated as follows for any value of the multiplication factor  $k_p$ . The contribution of generation  $i$  is obtained by convolving the normalized distribution  $P'(\tau)$  with itself  $i$  times and weighting the result by  $k_p^i$ .

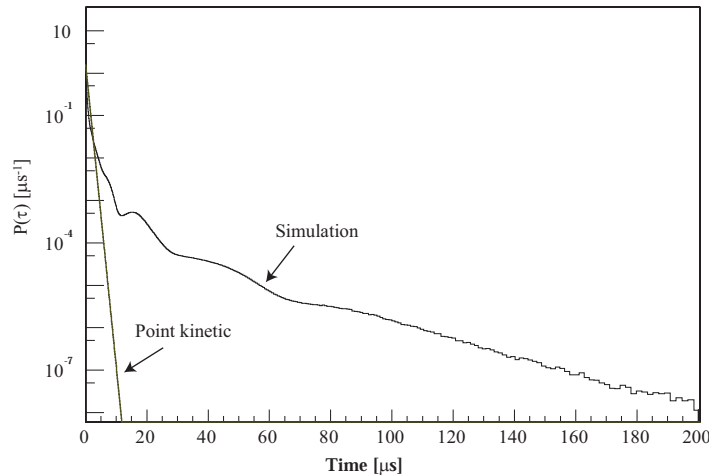


**Fig.3** Simulated intergeneration time distribution  $P(\tau)$  compared to the point kinetics prediction.

Then, for any value of the multiplication factor  $k_p$  we calculate the time dependence of the fission rate by summing the contributions of all the successive generations:

$$N_{k_p}(t) = k_p P' + k_p^2 P' \otimes P' + k_p^3 P' \otimes P' \otimes P' + \dots \quad (3)$$

Finally, for each value of the prompt multiplication coefficient, the logarithmic derivative  $\alpha_{k_p}(t)$  is calculated as a function of time.

The result of such a calculation is shown in Figure 4. For  $k_p$  values ranging from  $k_p = 0.95$  to  $k_p = 0.995$  by steps of 0.005 (reactivity change of 500 pcm).

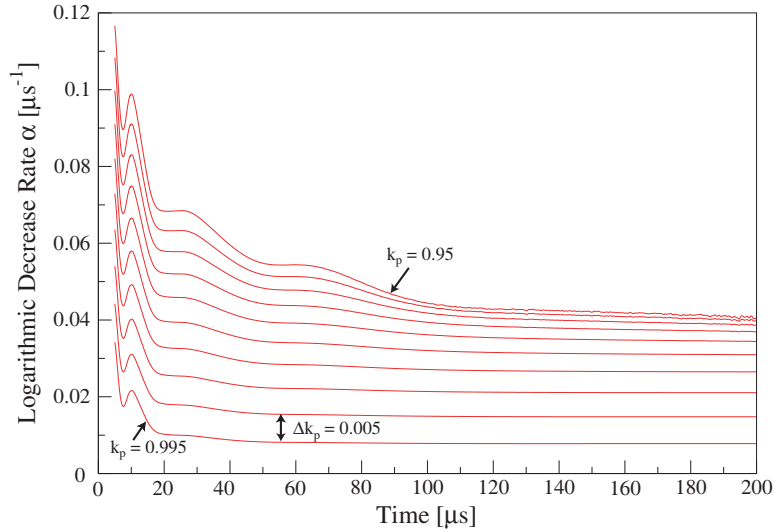


**Fig.4** Calculated logarithmic decrease rates as function of the time for several multiplication factors.

For any reactivity levels the curves corresponding to different  $k_p$  values are well separated on a time range of 80  $\mu\text{s}$ , thus demonstrating the power of the method for  $k_p$  determination. However, the asymptotic behavior of the slope parameter differs for the low and the high sub-criticality levels: for  $k_p$  values close to criticality, the curves corresponding to different  $k_p$  values are still well separated, but for  $k_p$  values below 0.97 all the curves are bunching together around a common value of the  $\alpha$  parameter ( $\alpha = 0.045 \mu\text{s}^{-1}$ ). This common behavior emphasizes the role of the reflector, which sends the neutrons back into the core after an average delay of 20  $\mu\text{s}$ . In the case of high sub-criticality configuration these “old” neutrons have a significant influence on the kinetics, due to the fast dying out of the first neutron generations.

The last characteristic one should notice is the wavy character of the grid, especially for measuring times lower than 50  $\mu\text{s}$ . A numerical tracking of the neutrons relates these undulations to the crossing of the various cross-section resonances by neutrons coming back from the reflector: for these neutrons, the reflector acts as a slowing down spectrometer, producing a correlation between their energy and the time spent in the reflector materials.

### 3.3 Results and Discussion

The analysis described in the preceding section was applied on the data shown in Figure 2. A least square adjustment of the experimental values  $\alpha_{\text{exp}}(t)$  to the corresponding  $\alpha_{k_p}(t)$  gives the value of the multiplication coefficient  $k_p$  we are looking for. The results are shown in Figures 5 for the SC0 core configuration and for SC2 and SC3 core configurations.

In any case the method successfully reproduces on a wide time range, the shape of the neutron population decay. For the SC0 configuration, the “best fit” curve is framed by the curves corresponding to a  $\pm 50$  pcm difference. All the experimental data points are located in between the two curves, thus illustrating the discrimination power of the method.

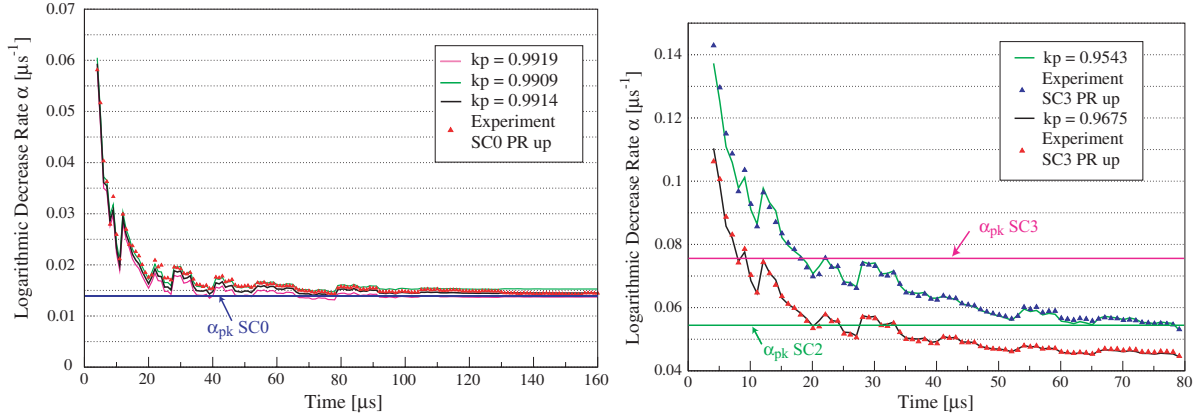


**Fig.5** Comparison of experimental and calculated logarithmic decrease rates for the SC0 configuration (left), and SC2, SC3 configurations (right). The point kinetics predictions are also displayed.

The results for the 6 experimental configurations are gathered in Table 1 and are compared to the values obtained by standard Source Multiplication (SM) methods used for the calibration. A perfect agreement is found between the two sets of data.

**Table 1** Results for the 6 experimental configurations compared to standard SM measurements (the  $k_p$  SM values are calculated using 320 pcm for  $\beta_{\text{eff}}$ ).

Core configuration	$k_p$ (this work)	$k_p$ (SM)
SC0 PR up	$0.9914 \pm 0.0005$	$0.9918 \pm 0.0005$
SC0 PR down	$0.9894 \pm 0.0005$	$0.9907 \pm 0.0005$
SC2 PR up	$0.9675 \pm 0.0010$	-
SC2 PR down	$0.9655 \pm 0.0010$	$0.9688 \pm 0.0030$
SC3 PR up	$0.9543 \pm 0.0010$	-
SC3 PR down	$0.9520 \pm 0.0010$	$0.9536 \pm 0.0070$

Finally to check the validity limits of the PK approximation, the constants  $\alpha_{\text{PK}}$  have been calculated and are plotted in Figures 5. These constants are calculated by inserting in equation (1) a prompt neutron lifetime  $l = 0.6 \mu\text{s}$ , obtained by a MCNP simulation. We clearly observe two different behaviors depending on the sub-criticality level: for the SC0 configuration, the neutron population decays faster than the PK expectation during the first tens of microseconds but reach an asymptotic value close to the PK prediction. By contrast, for the SC2 and SC3 configurations, the PK approximation fails to reproduce the  $\alpha_{\text{exp}}(t)$  values which exhibit a strong time dependence in the experimentally accessible time window. In this case, as we have seen in Figure 4, the asymptotic kinetics is governed by the reflector physical properties.

#### 4. Neutron Spectroscopy

In a sub-critical multiplying medium driven by a 14 MeV neutron source, the birth of neutrons takes place in the MeV energy range, where the competition between capture, elastic and inelastic collisions and even multiplicative ( $n, 2n$ ) reactions will determine the available neutron flux at lower energies. Being faced with such a complex process, we have to be sure that numerical simulations correctly reproduce observable quantities such as neutron energy distribution.

#### 4.1 Neutron Counter

The energy range between a few tens of keV and 1-2 MeV can be explored using  $^3\text{He}$  proportional counters. Neutrons entering such detectors interact with the  $^3\text{He}$  gas through the exothermic  $^3\text{He}(n, p)\text{T}$  reaction and through the elastic scattering:  $^3\text{He}(n, n)^3\text{He}$ . The detector is built as a stainless steel cylinder with an inner radius of 1 cm, the central anode is made of a 25  $\mu\text{m}$  stainless steel wire kept at 1700 V and giving a charge multiplication factor of 10 over a length of 6 cm. The counter is filled with a gas mixture of 6 bars of argon, 5 mbars of  $^3\text{He}$  and a few mbars of  $\text{CO}_2$  for avalanche quenching. The high pressure of argon is needed to reduce the range of the charged particles thus minimizing the wall and end effects. The choice of a low  $^3\text{He}$  partial pressure is dictated by the high neutron fluence encountered in the experiment which would lead to unwanted pile-up effects.

#### 4.2 Calibration of the Detector Response to Neutrons

The  $^3\text{He}$  counter response to mono-energetic neutrons was measured in a series of calibration experiments performed at the CEN Bordeaux-Gradignan (France) Van de Graaff accelerator. A monochromatic proton beam was sent on thin targets of metallic  $^7\text{Li}$ . For a fixed angle with respect to the proton beam, the (p, n) reaction produces a monochromatic neutron beam. The counter was irradiated with these neutrons at zero degree and the response function was directly measured. The detector was calibrated for neutron energies ranging from 0 to 1.5 MeV. The detector responses to mono-energetic neutrons were fitted and parameterized, the two reaction contributions being weighted according to their respective cross sections.

Figure 6 shows the response function of the counter to fast mono-energetic neutrons. The main peak on the right hand side corresponds to the full energy deposit which is the sum of the neutron kinetic energy and the (p, n) reaction Q value. Moving to lower energy there is a plateau produced by the partial charge collection brought about by wall effects. At lower energies there is an upward swing originating from elastic scattering on  $^3\text{He}$ .

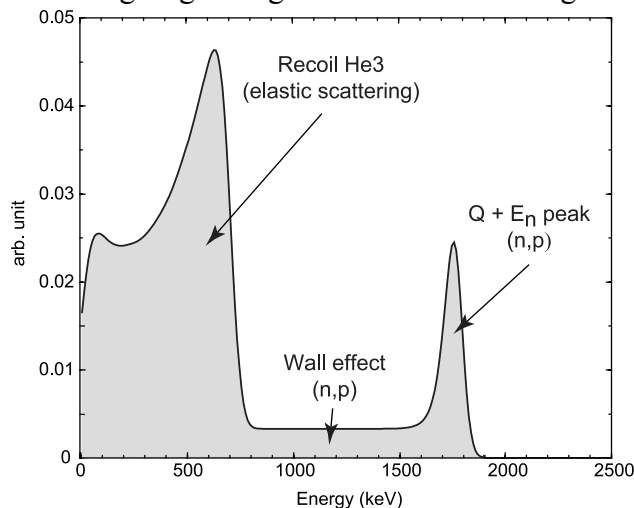


**Fig.6** Response spectrum of the  $^3\text{He}$  counter to 1 MeV monoenergetic neutrons (reconstructed from experimental response spectra).

#### 4.3 Experimental Procedure

The  $^3\text{He}$  counters were inserted into an axial channel in the center of the core region. The detectors were protected from gamma rays by a 2 cm thick lead shielding.

A first experiment [3] showed unexpected background events superimposed on the neutron signal in the MeV range of the spectrum. As Compton electrons cannot deposit such an energy in a few atm.cm of argon, these events must be attributed to charged heavy particles, namely alpha-particles or protons, resulting from (n,  $\alpha$ ) or (n, p) reactions on the structure materials of the counter. The rather low cross-sections for these reactions ( $10^{-3}$  b) are compensated by the large number of target atoms (Fe, Ni) located in the superficial layer of the counter wall, in direct contact with the active volume of the gas.

To evaluate this spurious event contribution we made a background measurement using a second proportional counter identical to the one used for spectroscopy but free of  $^3\text{He}$  active gas. This second measurement was subtracted from the  $^3\text{He}$  measurement, after normalization. The resulting spectrum, represented by the vector  $S$ , is related to the neutron energy spectrum  $\Phi$  through the matrix equation:

$$S = M \cdot \Phi. \quad (4)$$

$M$  is the convolution matrix provided by the calibration of the counter; each row of  $M$  corresponds to the spectrum of signals which would be produced by a mono-energetic neutron flux whose energy corresponds to the energy of the bin (see Figure 6).

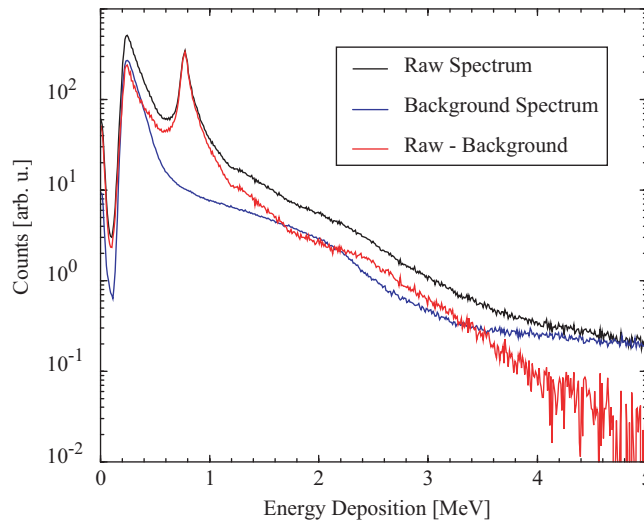


**Fig.7** Spectra measured in the fuel with the proportional counters with and without  $^3\text{He}$ , and spectrum obtained by subtraction of the background counting rate.

The neutron spectrum  $\Phi$  can be extracted by an iterative subtraction method [3] starting from the high energy end of the spectrum. Here the method is applied starting at 2.2 MeV and the result is shown in Figure 8. A Monte Carlo prediction (using the MCNP code) of the neutron energy distribution is also shown in this figure. We can see a rather good overall agreement from 50 keV up to 1.5 MeV. Below 50 keV no realistic spectrum is really expected as we are too close to the counter energy resolution, here 42 keV (FWHM). On the other hand the measured flux reproduces very well the dip predicted around 0.4 MeV which is due to the oxygen capture resonance. This differential measurement complements spectral indices and foil activation measurements which are based on threshold reactions and therefore giving access only to semi-integral flux values.

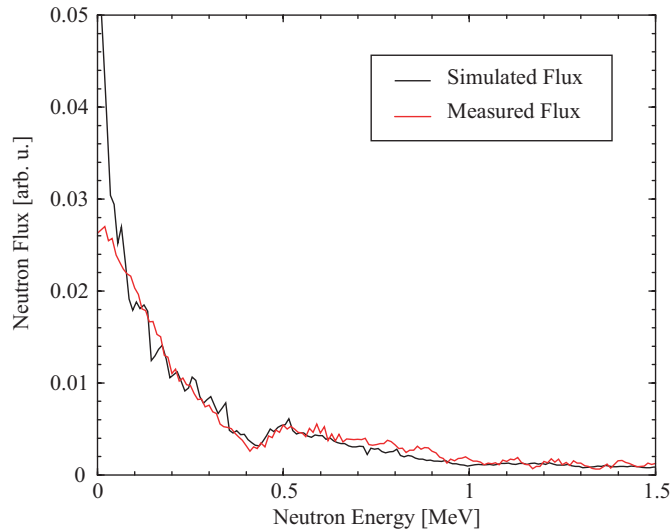


**Fig.8** Measured neutron flux compared to the flux simulated with MCNP.

## 5. Conclusion

In the MUSE project a pulsed deuteron generator was coupled to the MASURCA fast reactor to study the response of a subcritical assembly to an external source excitation.

We have developed a technique based on the analysis of the time decay of the neutron population which follows a neutron pulse. This technique enables us to take into account the full information contained in the PNS experiment with the help of a computer simulation of the intergeneration time distribution. This method suppresses the need to calibrate the reactivity on a critical configuration. As a consequence it can be used for the monitoring of a future ADS.

Concerning the neutron spectroscopy the  $^3\text{He}$  proportional counter measured the energy spectrum of the neutron fluence in the range of a few tens of keV up to about 1.5 MeV, after a deconvolution process of the collected signal spectra.

In spite of the many difficulties in performing such a measurement, a good agreement is found with the Monte Carlo prediction. Our measurements are unique because they cover the energy region where the shape of the distribution changes very rapidly and is very sensitive to the presence of neutron capture resonances. This gives us a direct test of the neutron transport understanding.

## Acknowledgements

We are very grateful to the CEA MASURCA reactor team and to the MUSE collaboration coordinator F.Mellier for their constant help. This work is partially supported by the 5<sup>th</sup> framework program of the European Commission (contract MUSE FIKW-CT-2000-00063).

## References

- 1) R.Soule, Int. Conf. PHYSOR 2002, October 7-10, Seoul, Korea, CD-Rom Proceedings, (ANS, 2002) 12C-01.
- 2) F.Perdu, A.Billebaud, R.Brissot, D.Heuer, C.Le Brun, E.Liatard, J.-M.Loiseaux, O.Méplan, E.Merle, J.Vollaire, "Prog. in Nucl. Energy, **42**, 107 (2002).
- 3) A.Billebaud, R.Brissot, D.Heuer, C.Le Brun, E.Liatard, J.-M.Loiseaux, O.Méplan, E.Merle, F.Perdu, J.Vollaire, C.Destouches, P.Chaussonnet, J.-M.Laurens, Int. Conf. PHYSOR 2002, October 7-10, Seoul, Korea, CD-Rom Proceedings, (ANS, 2002) 13C-01.